Integrating Coupled Inductor And Switched-Capacitor Based High Gain DC-DC Converter For PMDC Drive

1. K.Radhika,PG Student,2.C.Balachandra Reddy,Professor&HOD
Department of EEE,CBTVIT,Hyderabad

Abstract - This paper presents a integrating coupled inductor and switched-capacitor based high gain dc-dc converter for pmdc drive. The presented micro inverter operates with a constant off-time boundary mode control, providing MPPT capability and unity power factor. The proposed multi transformer solution allows using low-profile unitary turn's ratio transformers. Therefore, the transformers are better coupled and the overall performance of the micro inverter is improved. Due to the multiphase solution, the number of devices increases but the current stress and losses per device are reduced contributing to an easier thermal management. Furthermore, the decoupling capacitor is split among the phases, contributing to a low-profile solution without electrolytic capacitors suitable to be mounted in the frame of a PV module. The proposed solution is compared to the classical parallel-interleaved approach, showing better efficiency in a wide power range and improving the weighted efficiency.
Index Terms — AC-module, micro inverter, multiphase, photovoltaic.

I. INTRODUCTION

Material, energy, and information are the three important elements for human survival and development. Each new discovery for energy use transformed and greatly promoted the development of modern civilization:

- The invention of the steam engine brought us into the machine age.
- The invention and use of electricity brought us into the electrical age.
- The invention of the semiconductor transistor brought into the information age.
- The present renewable energy development and use will trigger a fourth industrial revolution of all the renewable energy use methods, photovoltaic power generation is a critical part of overall renewable energy development. According to the world energy organization predictions, as the traditional energy sources (such as coal, oil, and so forth) gradually dry up, renewable energy power generation will become a major energy method. Figure 1 shows the development trend of world energy.

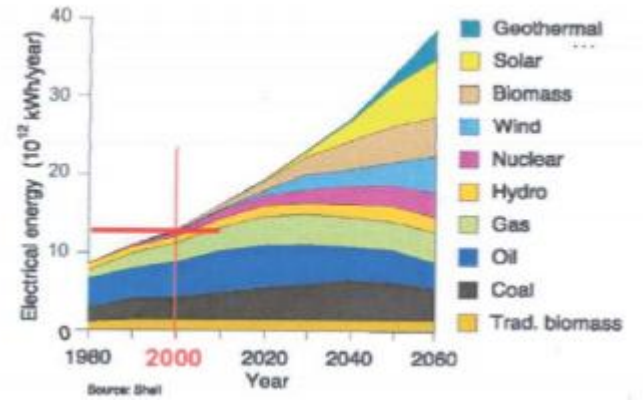

Fig.1

Governments are greatly concerned about the development of renewable energy. In 2007, the Chinese government issued a "renewable can meet the long-term development planning", and in 2008 issued a renewable energy development plan for the eleventh 5-year. According to the requirements of the plan, China photovoltaic power generation installed capacity in 2010 is 250 billion watts; it is estimated that by 2020 this capacity will reach 5000 billion watts, which, combined with the grid-tie photovoltaic power generation, accounts for 75 percent of the total. The main advantages of solar photovoltaic power generation include: Solar energy is abundant and inexhaustible.

- The material to product PV panels is widely distributed and abundant reserves
- Simple system structure, high conversion efficiency
- No pollution and can be recycle used
- Long life of photovoltaic battery, low maintenance costs
- Shortcomings of solar photovoltaic power generation include: Low power density, larger cover area
- Generation limited by natural conditions, no sun and no power High unit generating cost.

1.2 Classification Of The Photovoltaic Power Generation System

According to the application of the scene, photovoltaic generation system can be divided into the off-grid solar inverter system and the grid-tied solar inverter system. The off-grid solar inverter system is mainly used in composition-independent photovoltaic power generation system, applied in the family, the countryside, island, and remote areas of the power supply, and urban lighting, communications, testing and application of the system of power supply. Figure 2 is a system block diagram that shows the main components of the solar panels components, solar inverter units, energy storage unit, and electricity load and so on.

Fig.2

While the grid-tie solar inverter system is mainly used in parallel with the traditional utility grid, the solar inverter converts the energy from the PV panel to the traditional utility grid, the main components of the solar panels components, solar inverter units, smart bidirectional metering, the house's consumer load and traditional utility grid, and so forth (see Figure 3).

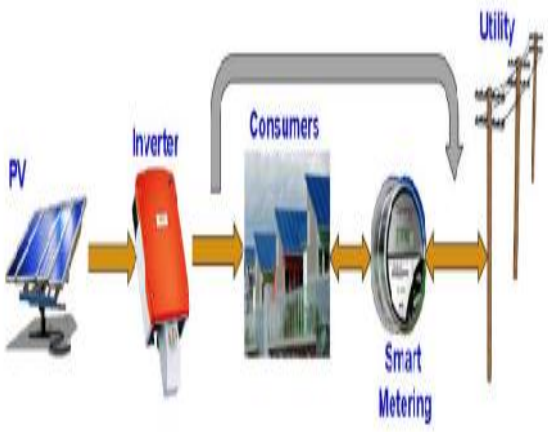

Fig.3

1.3 Solar Inverter Topology Shifts

Because the output voltage of one PV cell is from 20 to 45 volts with the change of illumination, if a higher output voltage is needed to suit for grid-tied application, usually consider putting a PV cell in parallel and in series to obtain high input voltage, and use one inverter to realize electric energy conversion. This type of topology is called "central inverters" just like Figure 5(a); its main feature is 10 to 250 kw, 3-phase and several strings in parallel

- High converter efficiency, low cost and low reliability
- Not optimal MPPT
- Usually used for power plants

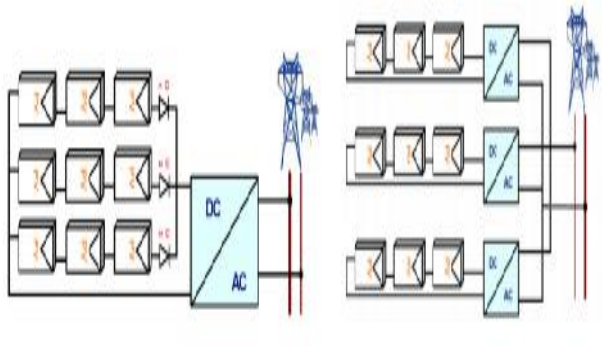

Fig.4

Another application is putting a PV cell in series to make the energy conversion, in every series branch. There is one MPPT module to capture maximum energy from the PV panel. This type of topology is called "string inverters" just like Figure 5(b); its main feature is: 1 to 10 kw, typical residential application

- Each string branch has its own inverter enabling better MPPT
- The strings can have different orientations
- Three-phase inverters for output power above 5 kw.

II. LITERATURE SURVEY

Single-phase grid-connected PV inverters present similarities with the power factor correction (PFC) application and control [20], power decoupling [21] strategies as well as topologies [22] from PFC have been adapted to PV inverters. A buck converter connected between the solar panel and the grid using an unfolder stage, thus working as a current source, is shown in Fig. 6. As in the boost converter in PFC applications, if the buck converter is operated in the boundary (BCM) between continuous (CCM) and discontinuous conduction mode (DCM) the injected current to the grid is proportional to the grid voltage (see Fig. 7). By analyzing the average current value in

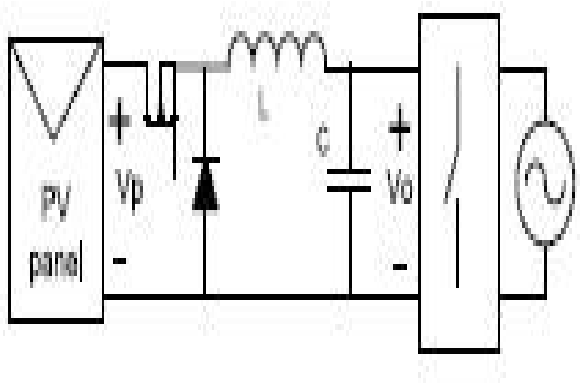

Fig. 6. Buck converter connected between a PV panel and the grid.

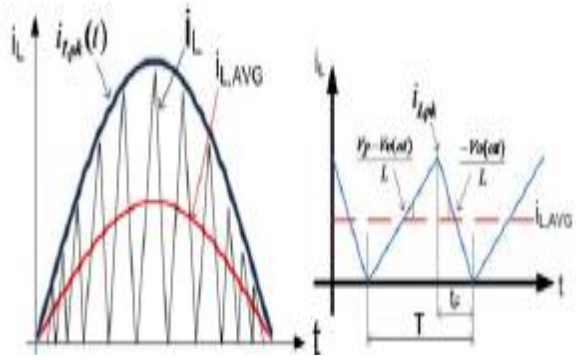

Fig. 7. Buck inductor current within a grid half-period and within a switching period.

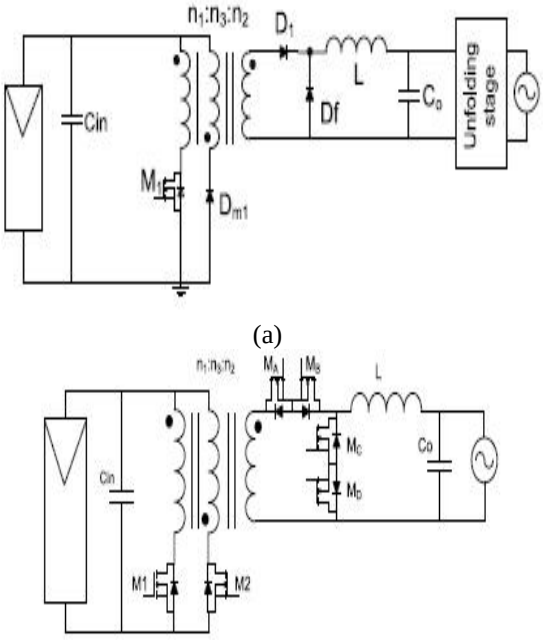

(a)

(b)

Fig. 8. (a) Proposed single-stage forward micro-inverter with unfolder stage and (b) with bidirectional secondary side switches.

a switching cycle, it can be concluded that this is possible if the off-time is kept constant (1)

$$i_{L,\mathrm{AVG}} = \frac{1}{2} \cdot i_{Lpk} = \frac{1}{2} \cdot \frac{Vo(\omega t)}{L} \cdot t_F = K \cdot Vo(\omega t), \text{if } t_F = \text{const.} \quad (1)$$

In the case of ac-module application, the input voltage is up to 50 or 100 V for crystalline silicon and thin-film modules, respectively [4]. As a consequence, a boosting transformer is necessary for grid interface, especially for the European grid voltage. Several isolated buck-derived topologies can be used. However, due to the low power range of the commercial PV modules, simple topologies as forward converter are preferred.

Two possible implementations are proposed for the single stage forward micro inverter, as shown in Fig. 8: a) with unfolding stage and b) with secondary side switches.

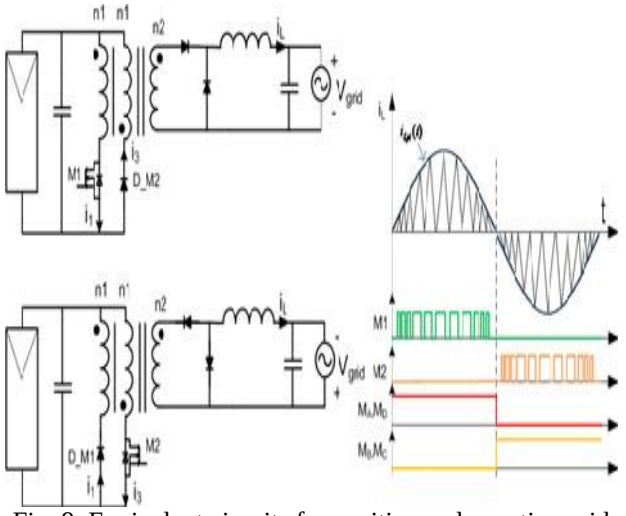

Fig. 9. Equivalent circuits for positive and negative grid voltage operation.

In both cases, the primary transistors are high-frequency switched to operate the micro inverter in the boundary mode. Implementation b) integrates the unfolding stage in the micro inverter power stage, i.e., the secondary side bidirectional switches are line frequency switched according to the grid voltage polarity. Thus, two sub circuits are generated as depicted in Fig. 9. Therefore, the two primary windings are used either for energy transfer or transformer reset during the corresponding grid half-cycle and the primary to tertiary turn`s ratio is forced to be the same. Furthermore, both primary windings are designed for the same current stress; hence, a bigger core is needed.

III. PROPOSED METHOD AND RESULTS

PRIMARY-PARALLEL SECONDARY-SERIES MULTICORE TRANSFORMER FORWARD MICROINVERTER

In the configurations presented in Fig. 8, the necessary primary to secondary turn`s ratio to achieve a proper interfacing between the low PV module voltage and the grid is large, thus the performance of the converter can be worsened. Fig. 10 shows the proposed multi core forward topology derived from the topology presented in Fig. 8(a), which consists of several highly coupled transformers which are parallel connected in the primary side and series connected in the secondary side.

The parallelization in the primary side reduces the current stress in both switches and primary windings of the transformer. The current sharing is guaranteed because of the secondary series connection, although affected by the coupling of the individual transformers. The current stress is also decreased in the secondary side diodes due to the common cathode configuration and the synchronized driving of the primary switches. As a result, SMD devices can be used, a low-profile implementation is feasible and the thermal management is improved, although more devices are needed.

The secondary series connection allows achieving the grid voltage using transformers of lower turn`s ratio. Therefore, the primary to secondary coupling at each transformer can be significantly improved, i.e.,

primary side current sharing is improved and parameters such as leakage inductance can be reduced, thus improving the off transition of the primary transistors.

3.1 Operation Principle, Voltage Gain and Transformers Turn`s Ratio

The primary switches are synchronized and sinusoidally modulated following the boundary mode control (BCM) strategy to

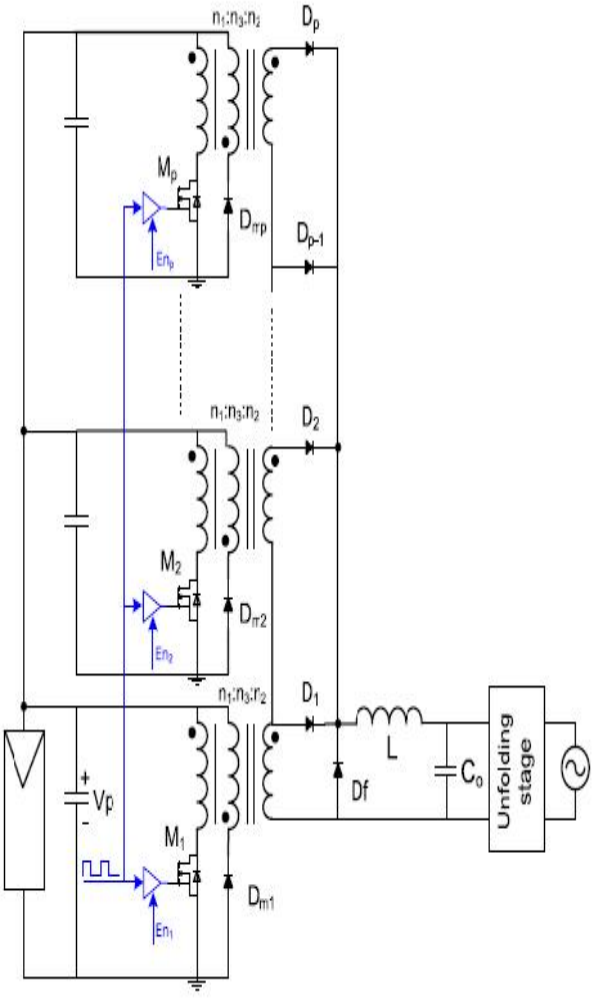

Fig. a

Proposed forward micro inverter topology with primary-parallel secondary-series-connected transformers. Generate a rectified sinusoidal current, which is unfolded in a line frequency switched bridge to inject unitary power factor current to the grid. Therefore, the application of the presented topology is intended for those grid connections where grid support is not demanded by the grid operator [23]. Furthermore, in order to comply with the harmonic requirements of the different standards [4], an EMI filter is necessary after the unfolding stage [24].

The high-frequency operation of the topology can be divided in two intervals as the classical forward converter operating in BCM. The main ideal waveforms of the proposed solution when two phases are active for a four-transformer inverter are shown in Fig. 6. As it can be observed, the common cathode configuration of the secondary diodes together with the synchronized control strategy make that only one of the secondary side diodes is in the current path at each moment. The number of active phases at each moment is decided according to the grid voltage as shown in Fig. 12 for the four-transformer inverter. As shown in the presented ideal waveforms, during the on time the voltage applied to the output filter is proportional to the number of active phases. During off-time, the inductor current flows through the free-wheeling diode in the same manner than in classical forward converter. Therefore, the voltage gain can be expressed as

$$V_o = n \cdot m \cdot d \cdot V_p \qquad (2)$$

where "*m*" is the number of active phases (e.g.,m = 2in Fig. 11), "*Vp*" the PV panel voltage, "*d*" the applied duty cycle and "*n*" is the primary to secondary turn`s ratio (*n*2 /*n*1) of each transformer, which is considered to be the same.

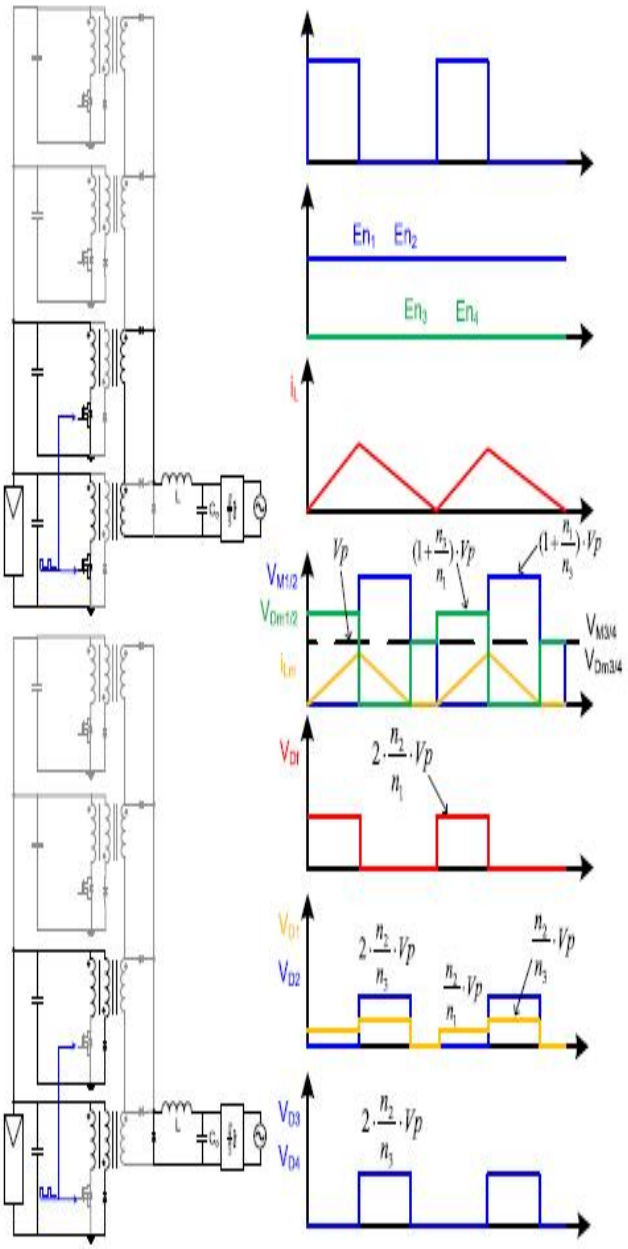

Fig. Ton and Toff configurations (left) and main waveforms (right) of the proposed converter when two phases are active.

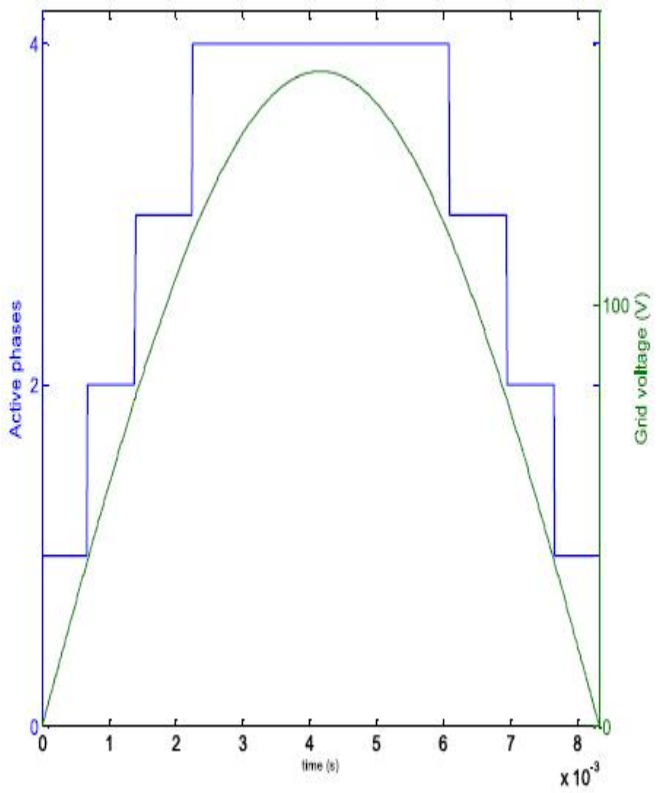

Fig. . Number of active phases during a line period for a four-transformer forward microinverter.

Using the presented voltage gain, the primary to secondary turn`s ratio of an individual transformer can be calculated as a function of the total number of transformers used "*p*" (e.g., *p* = 4 in Fig. 11), for a given solar module and a grid voltage (3)

$$n = \frac{n2}{n1} = \frac{Vo_{\text{peak}}}{p \cdot d_{\max} \cdot Vp_{\min}}. \quad (3)$$

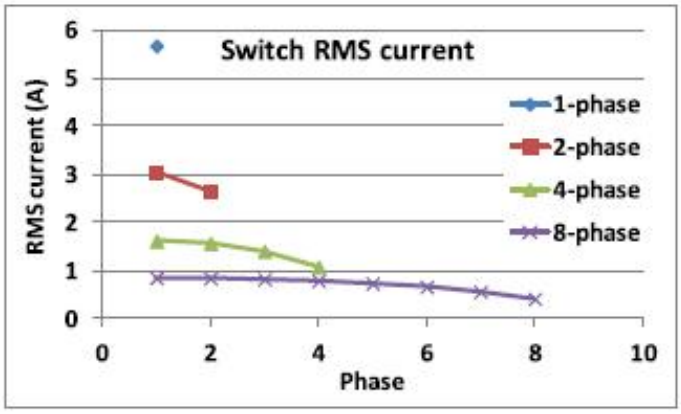

(a)

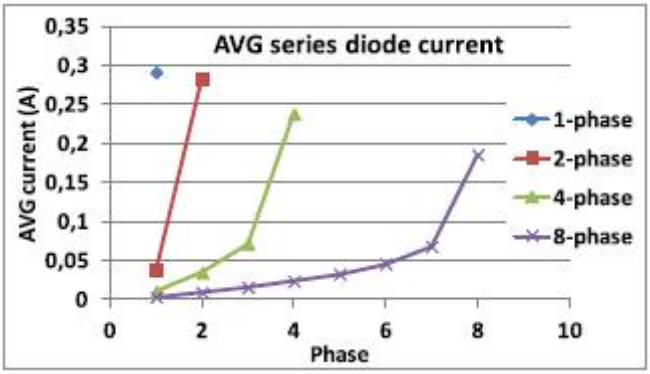

(b)

Fig. . (a) Primary switches rms current and (b) secondary series diodes AVG current during a grid period.

3.2 Inductor Value and Variable Frequency Operation

The applied BCM strategy ensures the injection of unity power factor current to the grid. However, the converter is operated with variable frequency and a trade-off between the chosen maximum frequency and the necessary inductance value (rms currents inside the circuit) must be achieved, for a given power level (4). With regard to the minimum operation frequency of the converter, it can be calculated as in (5), where "*p*" is the total number of phases

$$f_{\max} = \frac{V_{O\_\text{RMS}}^2}{2 \cdot L \cdot Po} \quad (4)$$

$$f_{\min} = \left(1 - \frac{V_{O\_pk}}{n \cdot p \cdot Vp}\right) \cdot f_{\max} \quad (5)$$

3.3 Component Stress

Since the operation of the proposed converter is the same than in a classical forward converter, the primary side component voltage stress in the proposed solution is also the same. However, the parallel operation of the converter reduces the current stress due to the current sharing, even more in the phases which are not active during the whole line period [see Fig. 13(a)].

With regard to the secondary side, only one of the series diodes (Di in Fig. 10) is in the current path at each moment due to the applied series configuration so the current stress is reduced in the secondary side diodes [see Fig. 13(b)]. The current stress of the free-wheeling diode remains the same regardless the number of transformers used.

The current stress reduction in both primary and secondary side components allows the utilization of SMD components, which provides advantages for the ac-module application such as thermal management or low-profile implementation. However, the increase in the number of components increases considerably the cost of the solution when the number of transformers is large. A qualitative cost comparison for the eight-transformer configuration respect to the single-transformer one is presented in the experimental results section.

The voltage stress for the freewheeling diode and the "*i*th" series diode of the secondary side can be

calculated according to (6) and (7), where "*p*" is the total number of transformers for the selected configuration

$$V_{\mathrm{KA\_FW}} = p \cdot \frac{n_2}{n_1} \cdot Vp \quad (6)$$

$$V_{\mathrm{KA\_Di}} = \max\left[(p-i)\cdot\frac{n_2}{n_1}\cdot Vp, i\cdot\frac{n_2}{n_3}\cdot Vp\right] \quad (7)$$

3.4 Semiconductor Losses Estimation

In the case of the primary switches, both the rms value and the voltage–current product when the switch is turned OFF are calculated at each switching cycle. Afterwards, those calculated values are used to compute the average in a line period. The same procedure is used for the mean values of the diode currents. The semiconductor losses can be calculated according to (8) and (9)

$$P_{\mathrm{Switch\_}i} = 1.6 \cdot R_{\mathrm{DSon}} \cdot \left(\frac{1}{k}\cdot\sum_{k,T_{\mathrm{grid}}} I_{Mi\_\mathrm{RMS}\_k}\right)^2 + \frac{1}{2}\cdot\left(\sum_{k,T_{\mathrm{grid}}} V_{\mathrm{OFF}\_i}\cdot I_{Mi\_pk}\right)\cdot \quad (8)$$

$$P_{\mathrm{Diode}\_j} = V_{F\_j}\cdot\frac{1}{k}\cdot\sum_{k,T_{\mathrm{grid}}} I_{Dj\_\mathrm{avg}\_k} \quad (9)$$

3.5 Input Capacitor (Line Frequency Power Decoupling)

In the proposed topology, the primary switches are synchronized and therefore there is no possibility to reduce the necessary input capacitance to filter the high-frequency ripple of the input current, as in interleaved converters. However, in the case of single-stage micro inverters, like the proposed in this paper, the input capacitance is designed to guarantee a proper balance between the demanded twice-line frequency current and the dc current provided by the PV module [21].A proper power balance allows low voltage ripple in the PV module in order to ensure a high maximum power point tracking (MPPT) efficiency. Due to the low voltage in the PV module, a large capacitance is required in parallel with the PV module (2 mF@45 V/120 W, for 8.5% of voltage ripple [25]), which is typically some orders of magnitude larger than the required capacitance for high-frequency filtering. As a consequence, in most of the cases an electrolytic capacitor is used, which is bulky and may reduce the life span of the solutions.

In the proposed topology, this capacitance is distributed among the paralleled primaries, thus reducing the capacitor of each phase. Therefore, low profile ceramic capacitors can be used, making the proposed configuration suitable for ac-module application.

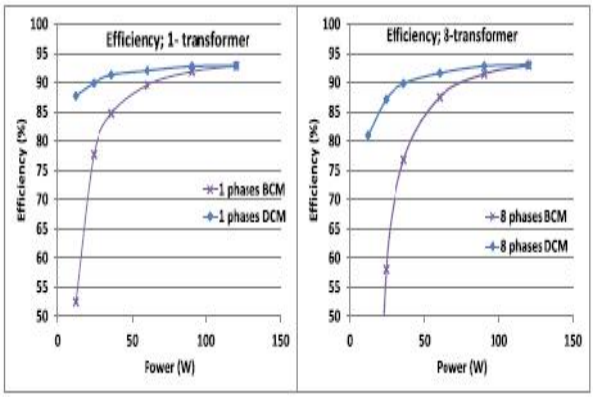

Fig. . Calculated efficiency for different configurations at DCM and BCM operation.

Simulink model

Extension Results

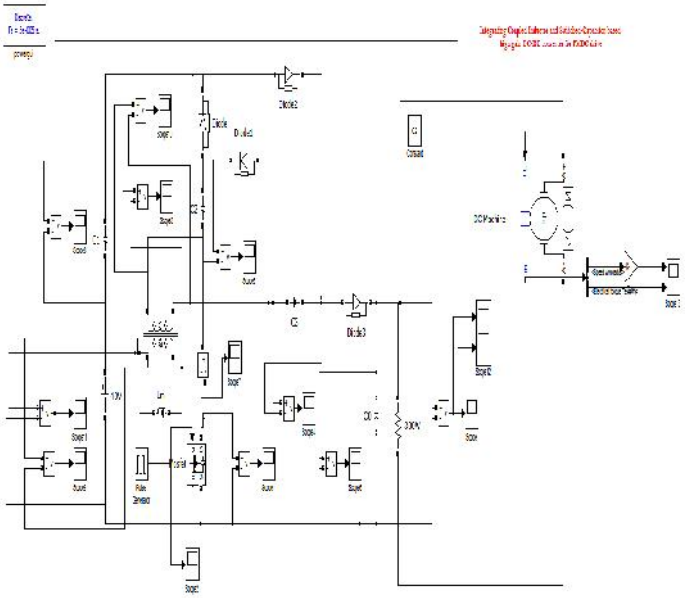

Fig. Circuit

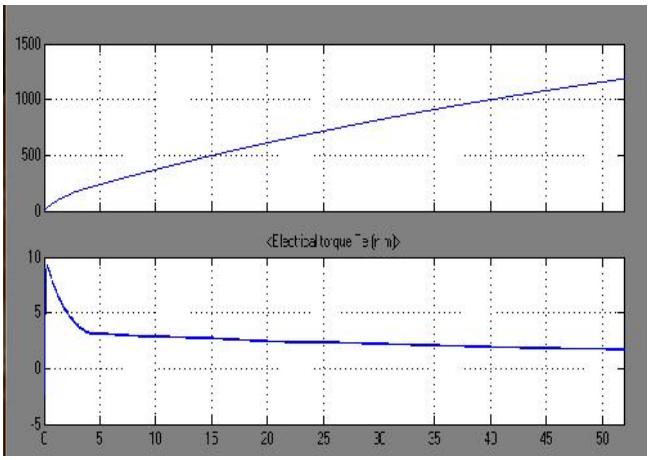

Fig. Electrical torque waveform

CONCLUSION

This paper introduces a multiphase primary-parallel secondary-series forward micro inverter operated in boundary and DCM, suitable for PV ac-module application. The key parameter is the number of transformers and its influence in terms of size, losses, leakage inductance, series resistance and resonance frequency of the transformers is explored. An increase in the number of transformers allows the utilization of better coupled transformers, improving the inverter performance. The total surface of the proposed solution increases with the number of transformers, however the height decreases making the solution suitable for PV ac-module application. DCM operation is introduced to overcome the performance degradation due to the increase in the operation frequency of BCM at light load. Based on the analysis, single transformer prototype as well as prototypes of 2 and 8 transformers were built. Both multi transformer inverters present the same weighted efficiency of 92.4%, improving the single-transformer inverter performance in around 2%. Despite in the proposed designs the inductor limits the height of both solutions, the low-profiled eight-transformer configuration allows using ceramic capacitors and offers better THD and thermal management capabilities, reducing the primary side temperature in 20 °C. The proposed parallel-series micro inverter is compared to a classical eight-transformer-interleaved forward micro inverter. The light-load efficiency is improved in the interleaved approach, but the single-transformer efficiency is slightly improved (less than 1%) and the CEC efficiency is lower than the parallel-series approach. The parallel-interleaved implementation presents a height reduction of 45% in respect to the parallel-series prototype, with an increase of 20% in area.

REFERENCES

[1] N. Femia, G. Lisi, G. Petrone, G. Spagnuolo, and M. Vitelli, "Distributed maximum power point tracking of photovoltaic arrays: Novel approach and system analysis," *IEEE Trans. Ind. Electron.*, vol. 55, no. 7, pp. 2610–2621, Jul. 2008.

[2] L. Quan and P. Wolfs, "A review of the single phase photovoltaic module integrated converter topologies with three different DC link configurations," *IEEE Trans. Power Electron.*, vol. 23, no. 3, pp. 1320–1333, May 2008.

[3] L.Wuhua andH.Xiangning, "Reviewof nonisolated high-step-upDC/DC converters in photovoltaic grid-connected applications," *IEEE Trans. Ind. Electron.*, vol. 58, no. 4, pp. 1239–1250, Apr. 2011.

[4] D. Meneses, F. Blaabjerg, O. Garca, and J. A. Cobos, "Review and comparison of step-up transformerless topologies for photovoltaic AC-module application," *IEEE Trans. Power Electron.*, vol. 28, no. 6, pp. 2649–2663, Jun. 2013.

[5] Z. Yi, L.Wuhua, D. Yan, and H. Xiangning, "Analysis, design, and experimentation of an isolated ZVT boost converter with coupled inductors," *IEEE Trans. Power Electron.*, vol. 26, no. 2, pp. 541–550, Feb. 2011.

[6] B. York, Y. Wensong, and L. Jih-Sheng, "An integrated boost resonant converter for photovoltaic applications," *IEEE Trans. Power Electron.*, vol. 28, no. 3, pp. 1199–1207, Mar. 2013.

[7] C. Dong, J. Shuai, F. Z. Peng, and L. Yuan, "Low cost transformer isolated boost half-bridge micro-inverter for single-phase grid-connected photovoltaic system," in *Proc. 27th Annu. IEEE Appl. Power Electron. Conf. Expo.*, Feb. 2012, pp. 71–78.

[8] C. Huang-Jen, L. Yu-Kang, Y. Chun-Yu, C. Shih-Jen, H. Chi-Ming, C. Ching-Chun, K. Min-Chien, H. Yi-Ming, J. Yuan-Bor, and H. Yung- Cheng, "A module-integrated isolated solar microinverter," *IEEE Trans. Ind. Electron.*, vol. 60, no. 2, pp. 781–788, Feb. 2013.

[9] A. Fernandez, J. Sebastian, M. M. Hernando, M. Arias, and G. Perez, "Single stage inverter for a direct AC connection of a photovoltaic cell module," in *Proc. 37th IEEE Power Electron. Spec. Conf.*, Jun. 2006, pp. 1–6.

[10] Z. Zhiliang, H. Xiao-Fei, and L. Yan-Fei, "An optimal control method for photovoltaic grid-tied-interleaved flyback microinverters to achieve high efficiency in wide load range," *IEEE Trans. Power Electron.*, vol. 28, no. 11, pp. 5074–5087, Nov. 2013

[11] H. D. Thai, J. Barbaroux, H. Chazal, Y. Lembeye, J. C. Crebier, and . Gruffat, "Implementation and analysis of large winding ratio transformers," in *Proc. 24th Annu. IEEE Appl. Power Electron. Conf. Expo.*, Feb. 2009, pp. 1039–1045.

[12] C. Daolian and L. Lei, "Novel static inverters with high frequency pulse DC link," *IEEE Trans. Power Electron.*, vol. 19, no. 4, pp. 971–978, Jul. 2004.

[13] A. Costabeber, P. Mattavelli, and S. Saggini, "Digital time-optimal phase shedding in multiphase buck converters," *IEEE Trans. Power Electron.*, vol. 25, no. 9, pp. 2242–2247, Sep. 2010.

[14] M. Fornage, "Method and apparatus for converting direct current to alternating current," U.S. Patent US 7 796 412 B2, Sep. 14, 2010.

[15] O. Ziwei, G. Sen, O. C. Thomsen, and M. A. E. Andersen, "Analysis and design of fully integrated planar magnetics for primary–parallel isolated boost converter," *IEEE Trans. Ind. Electron.*, vol. 60, no. 2, pp. 494–508, Feb. 2013.